

The Structure and Weak Ferromagnetism of the Double Layered Cuprocobaltate: $\text{Y}_2\text{SrCu}_{0.6}\text{Co}_{1.4}\text{O}_{6.5}$

R. K. Li,^{*,†} R. Kremer,^{*} and J. Maier^{*}

^{*}Max-Planck-Institut für Festkörperforschung, Heisenbergstraße 1, D-70569 Stuttgart, Federal Republic of Germany; and

[†]Department of Chemistry, University of Science and Technology of China, Hefei, Anhui 230026, People's Republic of China

Received March 16, 1999; in revised form May 5, 1999; accepted May 24, 1999

Rietveld refinement of the X-ray powder diffraction (XRPD) pattern confirms that $\text{Y}_2\text{SrCu}_{0.6}\text{Co}_{1.4}\text{O}_{6.5}$ is isostructural to $\text{Y}_2\text{SrCuFeO}_{6.5}$. Unlike its Fe-analog which is antiferromagnetic, $\text{Y}_2\text{SrCu}_{0.6}\text{Co}_{1.4}\text{O}_{6.5}$ behaves as a three-dimensional (3D) ferromagnet below $T_C = 385$ K with a spontaneous magnetic moment per formula unit of only $\mu_s = 0.07\mu_B$ extrapolated to $T = 0$ K. We concluded that this weak ferromagnetism (WFM) originates from *Dzyaloshinsky–Moriya* (D–M) spin canting mechanism based on the observation of T^2 dependence of the low-temperature magnetization. The electrical resistance of sintered samples shows an exponential dependence on temperature $\exp(T_0/T)^\alpha$ with $\alpha = 1/2$ in the 185–570 K temperature range, which indicates the conduction mechanism is within variable range hopping (VRH) regime with long-range Coulomb interaction between the carriers. $\text{Y}_2\text{SrCu}_{0.6}\text{Co}_{1.4}\text{O}_{6.5}$ does not show any significant magneto-resistance effect in the 200–400 K temperature range. © 1999 Academic Press

In an attempt to prepare the Co-analog of $\text{Y}_2\text{SrCuFeO}_{6.5}$, Li *et al.* found that single-phase samples can be prepared in the $\text{Y}_2\text{SrCu}_{1-x}\text{Co}_{1+x}\text{O}_{6.5}$ system within a narrow composition range ($0.3 \leq x \leq 0.5$) (5). Preliminary studies revealed that the X-ray powder diffraction (XRPD) patterns of the samples can be indexed with an orthorhombic lattice with cell constants close to those of $\text{Y}_2\text{SrCuFeO}_{6.5}$. Interestingly, contrary to its Fe-counterpart which shows AFM with $T_N = 265$ K (3), $\text{Y}_2\text{SrCu}_{0.6}\text{Co}_{1.4}\text{O}_{6.5}$ (composition studied for its best purity) was found to be ferromagnetic (FM) with a transition temperature of $T_C = 382$ K (5). The unexpected appearance of spontaneous magnetization and the possible relation of the present compound to the currently studied alkaline earth doped rare-earth cobaltates and mixed cupro-cobaltate which show giant-magnetoresistance (GMR) effect (6–8) motivated us to further investigate its structure and magnetic properties in more detail. The results from this investigation will be presented in this report.

INTRODUCTION

The intense search for new layered cuprates as potential high- T_C superconductors has also led to the discovery of many by-product compounds in which Cu in the CuO layers is substituted by other transition metal elements such as Co and Fe (1–4). Although the incorporation of such 3d ions may prevent the compounds from becoming superconductors, the study of the electron–electron interactions within the plane is of great interest for understanding the interaction in their high- T_C superconducting relatives. Those layered by-product compounds reported so far include YBaCuFeO_5 (1), $\text{YBa}(\text{Cu},\text{Co})_2\text{O}_5$ (2), $\text{Y}_2\text{SrCuFeO}_{6.5}$ (3), and $(\text{Y},\text{Ce})_n\text{SrCuFeO}_y$ ($n = 2, 3$) (4). Similar to most undoped parent compounds of the high- T_C superconductors, these compounds, in general, are antiferromagnetic (AFM). The structures of the above listed compounds all contain a direct apex-joining double pyramidal MO_5 ($M = \text{Cu}, \text{Fe}, \text{Co}$) layer. They can be related to the structure of $\text{YBa}_2\text{Cu}_3\text{O}_7$ or its derivative $(\text{R},\text{Ce})_2\text{Ba}_2\text{Cu}_3\text{O}_9$ by removal of the central BaCuO_2 chain unit.

EXPERIMENTAL

Samples of nominal composition $\text{Y}_2\text{SrCu}_{0.6}\text{Co}_{1.4}\text{O}_{6.5}$ were prepared by solid-state reaction from mixtures of Y_2O_3 , $\text{Sr}(\text{NO}_3)_2$, CuO , and Co_2O_3 at 980°C . Several intermittent grindings during calcination were necessary to achieve homogeneity in the final products. Powder X-ray diffraction patterns were recorded using a Rigaku r_B diffractometer equipped with a rotating anode source ($\text{CuK}\alpha$ radiation). A step scan with step-width 0.04° (2θ) and counting time of 5 s at each step were utilized to collect the intensity data in the 2θ range 15 – 125° . The magnetization measurements were performed with a SQUID magnetometer (MPMS, Quantum Design). The resistance of bar-shaped samples ($3 \times 3 \times 8$ mm³) was measured under both zero field and 6 T by the four-probe method. A current of 0.01 mA was applied for measurements at low temperature (185–400 K). At higher temperatures, 1 mA or 100 mA was applied.

RESULTS AND DISCUSSION

The Rietveld refinement of the X-ray powder diffraction pattern (DBWS-9411 package (9)) confirms the previous observation that $\text{Y}_2\text{SrCu}_{0.6}\text{Co}_{1.4}\text{O}_{6.5}$ is isostructural to $\text{Y}_2\text{SrCuFeO}_{6.5}$. The starting structural parameters for the refinement were taken from the reported values of $\text{Y}_2\text{SrCuFeO}_{6.5}$ (3). In total 42 parameters, including the structural parameters and others referring to background, surface roughness, preferred orientation, and Pearson peak profile function, were refined simultaneously and the refinement quickly converged to $R_{\text{wp}} = 7.2\%$, $S = R_{\text{wp}}/R_{\text{exp}} = 1.55$ (Fig. 1). The refined cell parameters and atomic positions are listed in Table 1. The good agreement between the calculated and experimental patterns also shows that the prepared samples are free of any XRD detectable impurity phases.

Magnetization from 400 to 4 K of $\text{Y}_2\text{SrCu}_{0.6}\text{Co}_{1.4}\text{O}_{6.5}$ powder sample under applied field of 0.1 T shows a spontaneous magnetization below a Curie temperature (T_C) of about 385 K (Fig. 2). The field dependence of the magnetization up to 5 T is shown in Fig. 3. At 400 K ($>T_C$), the paramagnetic behavior with linear field dependence is observed. At temperatures below T_C , the magnetization

TABLE 1
Refined Atomic Positions of $\text{Y}_2\text{SrCu}_{0.6}\text{Co}_{1.4}\text{O}_{6.5}$ at Room Temperature

| Atom | Wyckoff positions | x | y | z | B (\AA^2) |
|-------|-------------------|-----------|-----------|-----------|------------------------|
| Y | 16k | 0.2061(3) | 0.3616(2) | 0.1832(0) | 0.8(2) |
| Sr | 8j | 0.1974(4) | 0.3637(2) | 0 | 1.4(2) |
| Co/Cu | 16k | 0.7111(4) | 0.3843(2) | 0.0968(1) | 0.8(2) |
| O1 | 8j | 0.190(2) | 0.109(1) | 0 | 0.5(3) |
| O2 | 8i | 0 | 0.5 | 0.1035(8) | 1.0(4) |
| O3 | 4b | 0 | 0.5 | 0.25 | 0.6(6) |
| O4 | 8g | 0.5 | 0.277(1) | 0.25 | 1.0(4) |
| O5 | 16k | 0.440(2) | 0.2535(9) | 0.1084(5) | 1.9(3) |
| O6 | 8h | 0 | 0 | 0.3530(6) | 0.7(4) |

Note. Space group $Ibam$, $a = 5.4283(1)$ \AA , $b = 10.7274(2)$ \AA , $c = 19.9805(3)$ \AA , $R_{\text{wp}} = 7.20\%$, $S = 1.55$, $R_B = 4.05\%$.

increases rapidly at low field and then shows a linear dependence with larger applied magnetic fields ($m = m_{0H} + \chi H$), revealing its ferrimagnetic or most probably weak ferromagnetic (WFM, see below) nature. The residual magnetization m_{0H} values (also shown as dotted

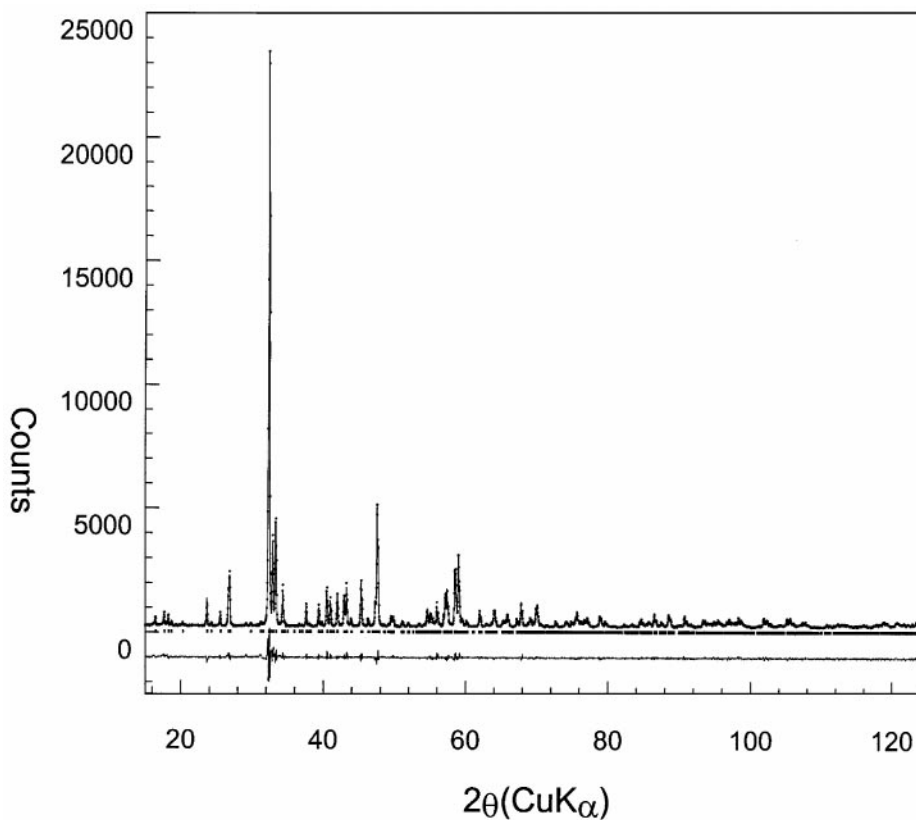


FIG. 1. Comparison of observed (dots), calculated (full line), and different (lower part) plots of the X-ray powder diffraction pattern of $\text{Y}_2\text{SrCu}_{0.6}\text{Co}_{1.4}\text{O}_{6.5}$, the vertical tick marks show the calculated reflection positions.

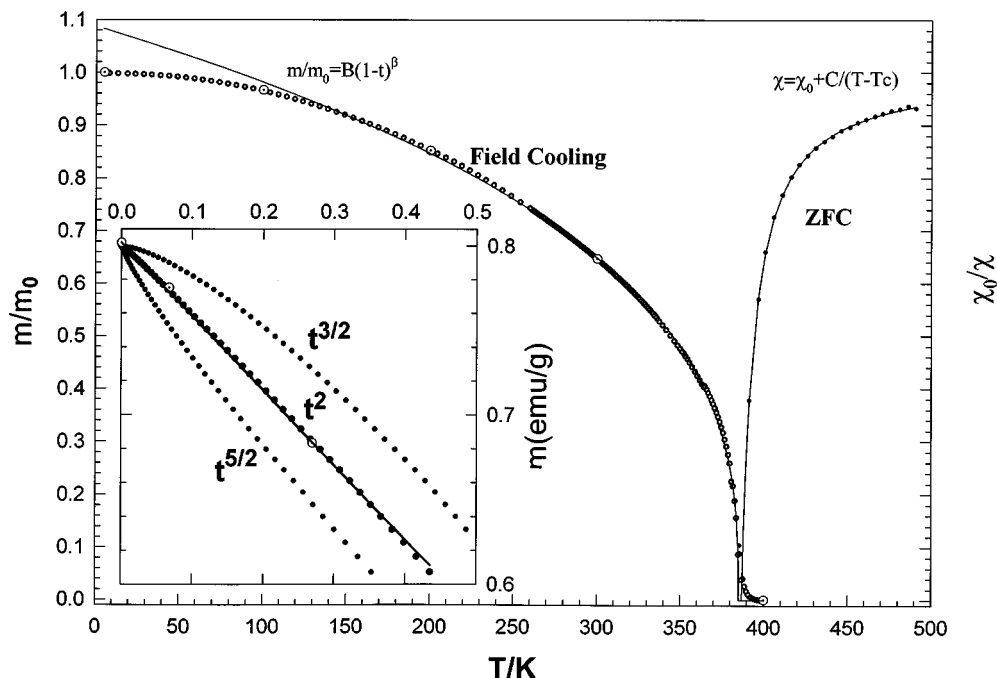


FIG. 2. Normalized magnetization (field cooling, left) and normalized susceptibility (right) of $\text{Y}_2\text{SrCu}_{0.6}\text{Co}_{1.4}\text{O}_{6.5}$. The magnetization curve was fitted to $m/m_0 = B(1-t)^\beta$ with $t = T/T_C$, $T_C = 385.1(1)$ K, $B = 1.087(2)$, $\beta = 0.342(1)$. The susceptibility curve was fitted to $\chi = \chi_0 + C/(T-T_C)$ with $\chi_0 = 2.856(9) \times 10^{-3}$ emu/mole, $C = 0.0211(2)$ emuK/mole, $T_C = 385.8(1)$ K. The inset shows linearity in a T^2 representation of low-temperature magnetization. It was fitted to $m/m_0 = 1 - at^2$ with $m_0 = 0.8019(3)$ emu/g, $a = 0.548(2)$. The larger dotted circles represent the zero field spontaneous magnetization obtained at 5, 100, 200, and 300 K.

large circles in Fig. 2) obtained by fitting the linear part of $M-H$ curves at different temperatures are also very close to those measured at the applied field of $H = 0.1$ T. The hysteresis loop of a piece of sintered sample with an arbitrarily fixed orientation at 300 K is also shown in Fig. 3 (inset) which again shows that the sample behaves like a ferromagnet. The coercive force, H_C , of the sample in this orientation is about 1.2 T and the remanent magnetization is about $M_r = 0.5$ emu/g at 300 K. The extrapolated spontaneous magnetization (from Figs. 2 and 3) at $T = 0$ K yields $m_0 = 0.8$ emu/g. This magnetization corresponds to a magnetic moment per formula unit of only $\mu_s = 0.07\mu_B/\text{f.u.}$, which is strongly reduced compared to the Cu^{2+} and Co^{2+} spin only effective Bohr magneton (μ_{eff}) in the paramagnetic states (the valence states of the corresponding ions are assigned as $\text{Y}_2^{3+}\text{Sr}^{2+}\text{Cu}_{0.6}^{2+}\text{Co}_{0.4}^{2+}\text{Co}_{1.4}^{3+}\text{O}_{6.5}$). Such a small μ_s value suggests that $\text{Y}_2\text{SrCu}_{0.6}\text{Co}_{1.4}\text{O}_{6.5}$ is very likely a weak ferromagnet.

By fitting the field warming magnetization (zero field cooled, Fig. 2, right panel) above the magnetic transition temperature T_C from 390 to 500 K with the modified Curie-Weiss law ($\chi = \chi_0 + C/(T-T_C)$, $\chi = M/H$) we obtained $T_C = 386$ K, $\chi_0 = 2.86 \times 10^{-3}$ emu/mole and $C = 0.02$ emuK/mol, which corresponds to $\mu_{\text{eff}}(\text{WFM}) = 0.4\mu_B$. The field cooled magnetization close to T_C from below can

be fitted with the scaling law

$$m/m_0 = B(1 - T/T_C)^\beta \quad T < T_C \quad [1]$$

Good agreement is obtained from T_C down to about 250 K (Fig. 2, left panel). The fit gives $T_C = 385$ K, which agrees well with the T_C value obtained in the paramagnetic range ($T > T_C$). The parameters of $B = 1.09$, $\beta = 0.34$ were also obtained from the same fit. The obtained β parameter is common to the experimental observations for three-dimensional ferromagnet and much larger than that for the 2D system (10). This finding may indicate that the transition at T_C is actually associated to the ordering of magnetic moments in the $(\text{Cu}/\text{Co})\text{O}_5$ planes interacting through the interlayer coupling across the $\text{Y}_2\text{O}_{1.5}$ fluorite layers.

In the low-temperature region, the magnetization can be fitted with the power law

$$m/m_0 = 1 - a(T/T_C)^2 \quad [2]$$

The fit gives good agreement (Fig. 2, inset) from 4 K up to about 230 K ($0.6T_C$) by using only two parameters m_0 and a . The square temperature dependence of magnetization also indicates Dzyaloshinsky-Moriya spin canting mechanism (11) of weak ferromagnetism. Ferrimagnetism from pos-

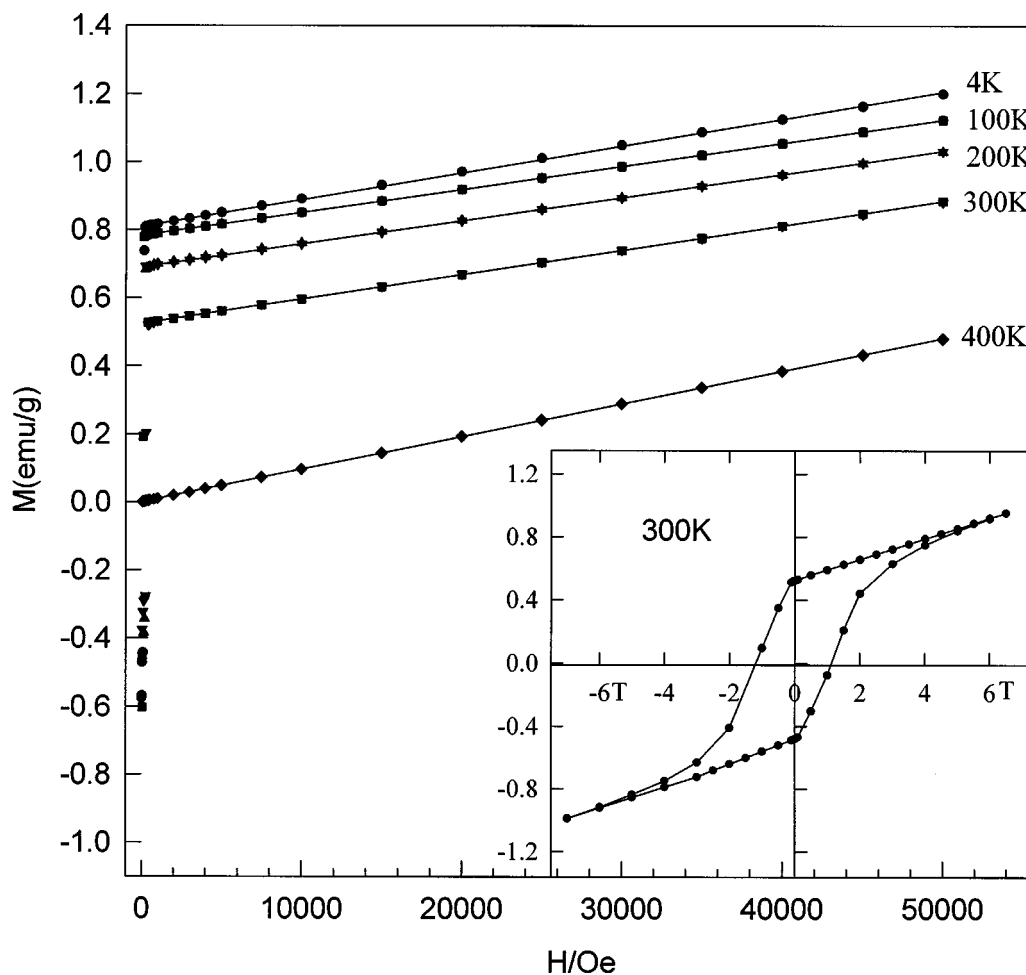


FIG. 3. Field-dependent magnetizations of $\text{Y}_2\text{SrCu}_{0.6}\text{Co}_{1.4}\text{O}_{6.5}$ at different temperatures. The straight lines represent the fits of the data to $m = m_{0H} + \chi H$. The inset shows the hysteresis loop of a sintered $\text{Y}_2\text{SrCu}_{0.6}\text{Co}_{1.4}\text{O}_{6.5}$ sample at an arbitrarily fixed orientation.

sible non-fully canceled moments of disproportional occupation of the Cu and Co ions in an ordered fashion can be ruled out from the relation as well, since in this case a $T^{3/2}$ dependence of magnetization will be observed according to standard spin wave theory for ferrimagnetism (12).

It can be shown that the D-M spin canting induced WFM is indeed allowed in the orthorhombic space group $Ibam$ adopted by present compound (13). The spin canting angle may be calculated by $\tan \theta = u_s(\text{WFM})/l_0$ ($l_0 = M_+ - M_-$, M_+ and M_- are the sublattice magnetization). It must be noted that the effective moment ($0.4 \mu_B/\text{f.u.}$) obtained from fitting the magnetization just above T_C (390–500 K range) cannot be used here as l_0 since it only reflects the magnetic moments contributed to WFM. As an estimate, we may take l_0 values of the Co and Cu ions from those of related compounds determined by neutron diffraction (14). It is found that the spin states of Cu, Co ions in the

pyramidal coordination are typically as $\text{Cu}^{2+}(1 \mu_B)$, $\text{Co}^{2+}(\text{high spin}, 3 \mu_B)$ and $\text{Co}^{3+}(\text{intermediate spin}, 2 \mu_B)$ (14), thus one obtains $l_0 = 3.8 \mu_B$ and $\theta \approx 1^\circ$. Unfortunately, we are unable to determine the actual canting direction due to lack of single-crystal measurements and magnetic structure details.

The resistance of a bar-shaped sample was measured from 1000 to 185 K as shown in Fig. 4. At high temperatures, namely, in the 375–1000 K range, the conductivity exhibits a semiconducting behavior with an activation energy of 0.33 eV as calculated from the slope of a $\log R$ vs $1/T$ plot. However, below 375 K the activation energy is seen to depend on temperature (e.g., 0.16 eV at 200 K), in agreement with the variable range hopping (VRH) conduction mechanism (15). In the temperature range between 185 and 400 K, the resistance can be reasonably well fit by a standard two-dimensional VRH conduction mechanism with $\log R$ vs $1/T^{1/3}$. However, we found that assuming a $\log R$ vs $1/T^{1/2}$

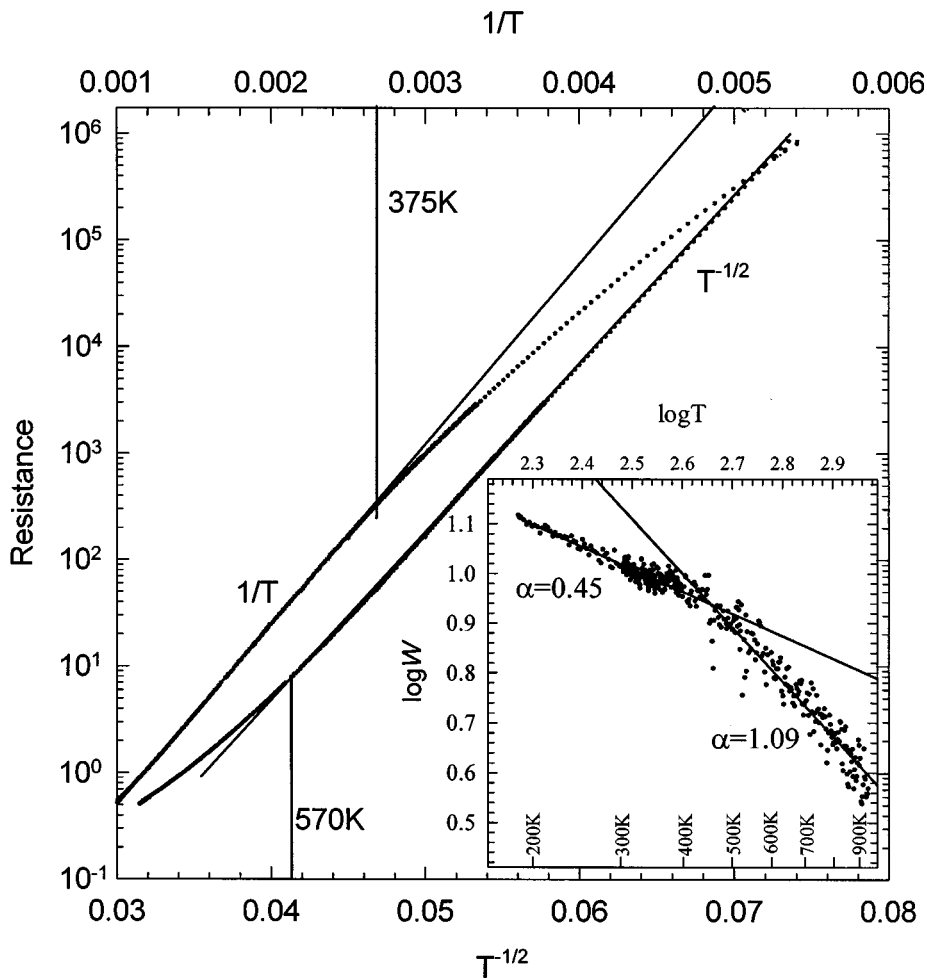


FIG. 4. Temperature dependent resistance of $\text{Y}_2\text{SrCu}_{0.6}\text{Co}_{1.4}\text{O}_{6.5}$ from 185 to 1000 K. The inset displays the $\log W$ vs $\log T$ ($W = d \ln R / d \ln T$) plot which clearly shows the change of slope (α) at about 400 K. Above 400 K, one gets $\alpha = 1.09(2)$ and below 400 K one gets $\alpha = 0.45(1)$ for $R = R_0 \exp(T_0/T)^\alpha$.

relation in the fit both improved the agreement of fit and extended the linearity range from 185 to 570 K with a resistance change over 5 orders of magnitude (Fig. 4). The latter relation of the resistance to temperature may be explained by the Efros and Shklovskii (ES) model which suggests (16):

$$\sigma = \sigma_0 \exp(-(T_0/T)^{1/2}), \quad [3]$$

with $T_0 = ne^2/\epsilon a$ where n is a numeric constant and a is the localization distance. ES mechanism in doped semiconductors and in oxides such as tungsten bronze is well established. It has previously been observed in some slightly doped high- T_C cuprates as well (17). However, those observations were limited to extremely low temperatures (< 10 K) except one report on $\text{PrBa}_2\text{Cu}_3\text{O}_7$ (18). According to this model, if the charge carriers are well localized and the long-range coulomb interaction must be taken into account

due to insufficient screening, it is argued that a soft Coulomb gap ($\delta E \propto (E - E_F)^2$) pinned at the Fermi level (E_F) will open up. This soft gap diminishes the density of states (DOS) near E_F leading to a crossover from Mott $\sigma = \sigma_0 \exp(-(T_M/T)^{1/4})$ variable range hopping regime (15) toward the above ES (Eq. [3]) dependence when lowering the temperature through a critical value $T_{ES} = e^4 N_0 a / \epsilon^2$ (N_0 is the noninteracting DOS). In normal doped semiconductors $N_0 \sim 10^{18} (\text{eV})^{-1}/\text{cm}^3$, $T_{ES} \sim 0.1$ K (16). For the present compound, the pyramidal coordination of the transition metal ions will stabilize the d_{z^2} orbital and the carriers are thus moving in the $d_{x^2-y^2}$ states of the Co^{2+} (HS) and Co^{3+} (IS) ions. The narrow $d_{x^2-y^2}$ band will lead to a much higher DOS at E_F , which can be well above $N_0 \sim 10^{22} (\text{eV})^{-1}/\text{cm}^3$ and result in a T_{ES} value of $T_{ES} \sim 1000$ K. This may explain the ES behavior observed below 570 K in $\text{Y}_2\text{SrCu}_{0.6}\text{Co}_{1.4}\text{O}_{6.5}$.

Alternatively, it is also possible to explain the temperature dependent resistance (Eq. [3]) by a model introduced by Sheng and Klafter to understand the conductivity of composite materials consisting of granular conducting particles embedded in an insulating matrix (19). They found that in a certain range of particle size and barrier potential one may also obtain the same relation (Eq. [3]) in a large temperature interval. However, for the present compound, it is found that Eq. [3] and its parameters persist for different annealing and sintering procedures, indicating that the Sheng and Klafter model may not be applicable for these samples.

CONCLUSION

The crystal structure of $Y_2SrCu_{0.6}Co_{1.4}O_{6.5}$ was established by Rietveld refinement of powder XRD data. Weak ferromagnetism with transition temperature of 385 K was observed from the magnetization measurements. Analysis of the magnetization behavior at low temperatures revealed that the weak ferromagnetism very likely originates from Dzyaloshinsky–Moriya spin canting. It is also observed that the temperature dependence of the sample resistance is in accordance to the Efros and Shklovskii model assuming a Coulomb gap opening at the Fermi level. However, no significant magneto-resistance effect was observed in this compound in the 185–400 K range.

ACKNOWLEDGMENTS

We thank Ms. Eva Brücher and Mr. S. B. Tang for experimental assistance. One of the authors (R.K.L.) thanks the Alexander-von-Humboldt foundation for a fellowship and Chinese Academy of Sciences for financial support.

REFERENCES

1. L. Er-Rakho, C. Michel, Ph. Lacorre, and B. Raveau, *J. Solid State Chem.* **73**, 531 (1988).
2. L. Barbey, N. Nguyen, V. Caignaert, H. Hervieu, and B. Raveau, *Mater. Res. Bull.* **27**, 295 (1992).
3. J. S. Kim, J. Y. Lee, J. S. Swinnea, H. Steinfink, W. M. Reiff, P. Lightfoot, S. Pei, and J. D. Jorgenson, *J. Solid State Chem.* **90**, 331 (1991).
4. R. K. Li, K. B. Tang, Y. T. Qian, and Z. Y. Chen, *Mater. Res. Bull.* **27**, 349 (1992).
5. R. K. Li, W. W. Xu, H. S. Yang, Y. B. Wang, Y. T. Qian, and Z. Y. Chen, *Mater. Res. Bull.* **29**, 1281 (1994).
6. G. Briceno, H. Chang, X. Sun, P. G. Schultz, and X. D. Xiang, *Science* **270**, 273 (1995).
7. C. Martin, A. Maignan, D. Pelloquin, N. Nguyen, and B. Raveau, *Appl. Phys. Lett.* **71**, 1421 (1997).
8. A. Maignan, R. Seshadri, C. Martin, F. Letouze, and B. Raveau, *Solid State Commun.* **102**, 551 (1997).
9. R. A. Young, S. Sakthivel, T. S. Moss, and C. O. Paiva-Santos, *J. Appl. Cryst.* **28**, 366 (1995).
10. S. T. Bramwell and P. C. W. Holdsworth, *J. Appl. Phys.* **73**, 6096 (1993).
11. I. E. Dzialoshinskii, *Sov. Phys. JETP* **6**, 1259 (1957); T. Moriya, in "Magnetism I" (G. T. Rado and H. Suhl, Eds.), p. 85. Academic Press, New York, 1963.
12. S. V. Vonsovskii, "Magnetism," Chap. 22, p. 825. Wiley, New York, 1974.
13. E. A. Turov, "Physical Properties of Magnetically Ordered Crystals." Academic Press, New York, 1965.
14. L. Barbey, N. Nguyen, V. Caignaert, F. Studer, and B. Raveau, *J. Solid State Chem.* **112**, 148 (1994).
15. N. F. Mott and E. A. Davis, "Electronic Processes in Non-Crystalline Materials." Clarendon Press, Oxford, 1979.
16. A. L. Efros and B. I. Shklovskii, *J. Phys. C* **8**, L49 (1975).
17. M. Z. Cieplak, S. Guha, H. Kojima, P. Lindenfeld, G. Xiao, J. Q. Xiao, and C. C. Chien, *Phys. Rev. B* **46**, 5536 (1992).
18. P. Bernstein, J. Bok, and A. Zylbersztejn, *Solid State Commun.* **70**, 271(1989).
19. P. Sheng and J. Klafter, *Phys. Rev. B* **27**, 2583 (1983).